Irrigation, damming, and streamflow fluctuations of the Yellow River

Zun Yin[1,2], Catherine Ottlé[1], Philippe Ciais[1], Feng Zhou[3], Xuhui Wang[3], Polcher Jan[2], Patrice Dumas[4], Shushi Peng[3], Laurent Li[2], Xudong Zhou[2,5,6], and Shilong Piao[3]

[1]Laboratoire des Sciences du Climat et de l'Environnement, IPSL, CNRS-CEA-UVSQ, Gif-sur-Yvette, France
[2]Laboratoire de Météorologie Dynamique, IPSL UPMC/CNRS, Paris 75005, France
[3]Sino-French Institute for Earth System Science, College of Urban and Environmental Sciences, Peking University, Beijing 100871, China
[4]Centre de Coopération Internationale en Recherche Agronomique pour le Développement, Avenue Agropolis, 34398 Montpellier CEDEX 5, France
[5]Institute of Industrial Science, The University of Tokyo, Tokyo, Japan
[6]State Key Laboratory of Hydrology-Water Resources and Hydraulic Engineering, Center for Global Change and Water Cycle, Hohai University, Nanjing 210098, China

Correspondence to: Z. Yin
(zun.yin@foxmail.com)

Abstract. The streamflow of the Yellow River is strongly affected by human activities of irrigation and dam regulation. Many attribution studies focused on the long-term trend of discharge, yet the contributions of these anthropogenic factors to stream-flow fluctuations have not been well quantified. This study aims to quantify the roles of irrigation and artificial reservoirs in monthly streamflow fluctuations of the Yellow River from 1982 to 2014 by using the global land surface model ORCHIDEE

5   with a new developed irrigation module, and a separate offline dam operation model. Validation with obsevations demonstrates the ability of our model in simulating the main hydrological processes under human disturbances in the Yellow River basin. Irrigation is found to be the dominant factor leading to 63.7% reduction of the annual discharges. It might lead to discharge increase in the summer if irrigation is widely applied during a dry spring. After illustrating dam regulation as the primary driver affecting streamflow seasonality, we simulated the changes of water storages in several large artificial reservoirs by a

10   new developed dam model, which does not require any prior knowledge from observations but only implements two simple operation rules based on their inherent regulation capacities: reducing peak flows for flood control and securing base flows during the dry season. Inclusion of dams with this simplified model substantially improved the simulated discharge by at least 42%. Moreover, simulated water storage changes of the LongYangXia and LiuJiaXia dams coincide well with observations with a high correlation value of about 0.9. We also found that the artificial reservoirs can affect the inter-annual fluctuations of

15   the streamflows, which however was not reproduced faithfully by our dam model due to lack of annual operation rules. From

the mismatches between simulations and observations, we inferred the potential impacts of multiple medium reservoirs and five large irrigation districts (e.g., the Hetao Plateau), which were ignored in most previous hydrological studies.

1 Introduction

More than 60% of rivers all of the world are disturbed by human activities (Grill et al., 2019) contributing to approximately 63% of surface water withdrawal (Hanasaki et al., 2018). River water is used for agriculture, industry, drinking water supply, and electricity generation (Hanasaki et al., 2018; Wada et al., 2014), these usages being influenced by direct anthropogenic

5   drivers and by climate change (Haddeland et al., 2014; Piao et al., 2007, 2010; Yin et al., 2020; Zhou et al., 2019). In order to meet the fast-growing water demand in populated areas and to control floods (Wada et al., 2014), reservoirs have been built up for regulating the temporal distribution of river water (Biemans et al., 2011; Hanasaki et al., 2006) leading to a massive perturbation of the variability of river discharges. In the mid-northern latitudes regions where a decrease of rainfall is observed historically and projected by climate models (Intergovernmental Panel on Climate Change, 2014), water scarcity will be further

10 exacerbated by the growth of water demand (Hanasaki et al., 2013) and by the occurrence of more frequent extreme droughts (Seneviratne et al., 2014; Sherwood and Fu, 2014; Zscheischler et al., 2018). Thus how to adapt and improve river management under different challenges is a crucial question for sustainable development, which requires comprehensive understanding of the impacts of human activities on river flow dynamics particularly in regions under high water stress (Liu et al., 2017; Wada et al., 2016).

15 The Yellow River is the second longest river in China. It flows across arid, semi-arid, and semi-humid regions, and it covers intensive agricultural zones containing about 107 million inhabitants (Piao et al., 2010). With 2.6% of total water resources in China, the Yellow River Basin (YRB) irrigates 9.7% of the croplands of China (http://www.yrcc.gov.cn). More importantly, underground water resources only accounts for 10.3% of total water resources amount in the YRB, outlining the importance of river water for regional water use. A special feature of the YRB is the huge spatio-temporal variation of its water balance.

20 Precipitation concentrates in the flooding season (from July to October) contributing to ~60% of annual discharge, whereas the dry season lasts from March to June accounting for ~10-20%. Numerous artificial reservoirs have been built up to regulate the streamflow intra- and inter-annually in order to control floods and alleviate water scarcity (Liu et al., 2015; Zhuo et al., 2019). The river discharge is thus highly controlled by human water withdrawals and dam operations, making it difficult to separate the impacts of human and natural factors on the discharge variability and trends.

25 Numerous studies assessed the effects of anthropogenic factors on streamflows and water resources in the YRB. By applying a distributed biosphere hydrological model in the YRB, Tang et al. (2008) quantified the contributions of climate change and human activities (irrigation and land cover change) to the annual discharge of the Yellow River at different reaches, and revealed the importance of human activities in influencing the low flow. Following studies confirmed anthropogenic impacts as the dominant factor affecting the trend of Yellow River discharge through modelling comparison or data analysis (Liu and

30 Du, 2017; Liu et al., 2019; Xi et al., 2018). Moreover, Yuan et al. (2018) investigated human-induced local climate change and demonstrated that its impact on extreme streamflows may be largely underestimated. The YRB is one of the major concerns of many global studies as well. For instance, studies from Haddeland et al. (2014); Hanasaki et al. (2018); Wada et al. (2014, 2016) analyzed potential human and climate impacts on the water resources of the YRB. But at the same time, they pointed

out the difficulty in simulating Yellow River discharge due to large intra- and inter-annual climate variability and complicated human activities.

Although those efforts indeed enhanced our understanding to the interactions among human, water resources, and climate change in the YRB, most of them only focused on the attributions to the long-term trend at annual and decadal scales. How
5 human activities affect intra-annual fluctuations of the streamflow is still not well clarified or quantified, which may mainly affect policies and regional economic activities. Moreover, the impacts of dam operations, as a key factor affecting discharge seasonality, are not well isolated from other anthropogenic effects in the studies of the YRB. The dam models in many studies are based on the work of Hanasaki et al. (2006), which simulates dam operations based on different purposes of reservoirs with adjustment to climate variation. This model requires observations to assess the mean annual discharge, and storage capacities
10 of reservoirs are only used to constrain the water storage. However, in reality, the operation target does not fully depend on water demands, but rely on the size of the reservoir (maximum regulation capacity) and the magnitude of the river discharge. More importantly, the simulated dam operations are hidden in the analysis with lack of validation by observations.

Many model studies are able to provide reliable estimation of river discharges but related physical processes are not fully represented. For instance, some model studies require extra observed data as inputs (e.g., leaf area index (LAI), evapotranspira-
15 tion, etc). Moreover, many biophysical processes (e.g., photosynthesis, LAI dynamics, crop phenology), which tightly couple with evapotranspiration, surface energy balances, and irrigation demands, are rarely considered in Global Hydrological Models (GHM). These missing processes are not important for hydrological studies using historical data and short-term forecast. However, they are probably non-negligible for long-term projections in regions where ecosytems react strongly to climate change through the hydrological cycle (de Boer et al., 2012; Lian et al., 2020; Zhu et al., 2016).

20 In a previous study, Xi et al. (2018) used the land surface model ORCHIDEE (ORganizing Carbon and Hydrology in Dynamic EcosystEms) to attribute the trends of main China's river streamflows to several natural and anthropogenic factors. Due to lack of representation of crop and irrigation processes, simulated results are consistent to the naturalized discharges of the Yellow River, however much higher than the real observations. By developing a new crop-irrigation module in ORCHIDEE (Wang et al., 2016; Wang, 2016; Wu et al., 2016; Yin et al., 2020), we were able to provide precise estimation of crop phenology,
25 yield and irrigation amount at both local and national scale in China (Wang et al., 2017; Yin et al., 2020). More importantly, ORCHIDEE-estimated irrigation accounts for potential ecological and hydrological impacts (e.g., physiological response of plants to climate change and short term drought episodes on soil hydrology) with respect to other land surface models and global hydrological models. Simultaneously, a simple dam operation model was developed to simulate the change of water storages in the main artificial reservoirs. Different from many dam models, it does not require any prior information from
30 observation. The dam regulation simulation is based on a targeted operation plan, which relies on the regulation capacity of the reservoir and historical simulated discharge, with flexibility to climate variation. The role of artificial reservoirs on streamflows could then be studied, and isolated from the effect of climate variability and irrigation trends. Moreover, different from classical approaches separating the YRB into up, middle, and down streams (Tang et al., 2008; Zhuo et al., 2019), we propose to further divide both the up and middle streams into sub-sections based on the locations of four key gauging stations (Fig. 1). This

Hydrology and
Earth System
Sciences
Discussions

Open Access

EGU

approach splits the regions with/without big reservoirs (or large irrigation areas) in the up and middle streams, which simplifies the assessment of the roles of irrigation and damming on discharge disturbances of the Yellow River.

Before its implementation in ORCHIDEE, the dam model should be validated offline. In this study, both ORCHIDEE and dam model are applied on the Yellow River from 1982 to 2014 in order to: 1) validate the performances of the new

5 crop-irrigation module and the dam model in simulating hydrological cycles and river discharge; and 2) qualify and quantify the impacts of irrigation and dam regulation on the fluctuations of monthly discharge. We first introduce the ORCHIDEE model and the simple dam model in Sect. 2.1. Then the algorithm estimating sub-sectional water balances is described in Sect. 2.2, followed by datasets, simulation protocol, and metrics for evaluation in Sect. 2.3-2.5. Results are shown in Sect. 3 and limitations are discussed in Sect. 4.

2 Methodology

10

2.1 Modelling irrigation and dam regulation

2.1.1 Irrigation in ORCHIDEE

Irrigation amount is simulated in the land surface model ORCHIDEE-CROP (Wang, 2016; Wang et al., 2017) as the minimum between plant water requirements and stream water supply. The irrigation module was designed and developed for the main

15 irrigated crops grown in China, i.e., wheat, maize, and rice. The plant water requirements are defined according to the choice of an irrigation technique, namely minimizing soil moisture stress for flooding, sustaining plant potential evapotranspiration for dripping, and maintaining the water level above the soil surface during specific months for paddy irrigation. Each crop being grown on a specific soil column (in each model grid-cell) where the water and energy budgets are independently resolved. Streams only supply water to the crops growing in the grid-cell they cross, according to the river routing scheme of the

20 ORCHIDEE-CROP model (Ngo-Duc et al., 2007). Since reservoirs are not modelled, irrigation may be underestimated where reservoirs regulation stores water in months without irrigation demand to be released it in months with irrigation demand. Transfer from reservoirs, lakes or local ponds to adjacent cells are not considered which should further lead to an underestimation of irrigation demand, dependent on the cell size. Details of the coupled crop-irrigation module of ORCHIDEE are fully described in Yin et al. (2020).

25 #### 2.1.2 Dam regulation model

To account for the impacts of dam regulation on stream flow (Q) seasonality, we developed a dynamic dam water storage module based on only two simple rules, reducing flood peaks and guaranteeing baseflow. This simple module depends on inflows only and is thus independent from irrigation demands. It has been developed for the main reservoirs of the YRB, (e.g., LongYangXia, LiuJiaXia, and XiaoLangDi) to assess the effect of water management rules on discharge. Different from

30 Biemans et al. (2011); Hanasaki et al. (2006), we primarily consider the ability of reservoirs in regulating river flow seasonality. It means that the targeted baseflow and flood control of our model are not fixed proportions of mean annual discharge, but

depends on the regulation capacity of reservoirs (C_{max}). Firstly, multi-year averaged monthly discharge (Q_{s}) is calculated based on simulations. To include the potential impacts of climate change on reservoir regulation, here we only consider the latest past 10-year simulations and give higher weight to closer year, as:

$$Q_{\mathrm{s},i} = \frac{\sum\limits_{j}^{j \in N} Q_i^j}{\sum\limits_{j}^{j \in N}}.$$ (1)

5   Here $Q_{\mathrm{s},i}$ [m^3.s^{-1}] is multi-year averaged monthly discharge of month i; j is year index; N is number of year accounted; For a upcoming year j, we only use the historical simulations (maximum latest ten years) to calculate Q_{s}.

    Secondly, we evaluate the targeted water storage change ΔW_{t} and monthly discharge Q_{t} considering the regulation capacity of each reservoir. As shown in Fig. S1, one year can be divided into two periods by comparing Q_{s} with $\bar{Q}_{\mathrm{s}}$. The longest continuous months with $Q_{\mathrm{s}} > \bar{Q}_{\mathrm{s}}$ is the recharging season for reservoirs, and the rest is the releasing season. The amount

10   of water stored during the recharging season (blue region in Fig. S1), which is determined by C_{max}, will be used during the releasing season (red regions in Fig. S1). The ΔW_{t} and Q_{t} can be estimated by:

$$k = \min\left(\frac{C_{\mathrm{max}}}{\alpha \sum\limits_{i}^{i \in \mathrm{Recharge}} Q_{\mathrm{s},i}}, k_{\mathrm{max}}\right),$$ (2)

$$\Delta W_{\mathrm{t},i} = k\alpha \left(Q_{\mathrm{s},i} - \bar{Q}_{\mathrm{s}}\right) + \bar{Q}_{\mathrm{s}},$$ (3)

$$Q_{\mathrm{t},i} = Q_{\mathrm{s},i} - \Delta W_{\mathrm{t},i}/\alpha.$$ (4)

15   Here k [-], varying between 0 and k_{max} (=0.7), indicates the ability of reservoir in disturbing discharge seasonality. It is a ratio of the maximum regulation capacity of the reservoir C_{max} [10^8 m^3] over the discharge amount during the recharging season. α (0.0263) converts monthly discharge to water volume. Assuming that the water storage of the reservoir reaches C_{max} at the end of the recharging season, we can calculate targeted water storage W_{t} by using ΔW_{t}.

    Finally, the actual water storage change of the reservoir ΔW is a decision regarding actual monthly discharge, current water

20   storage, Q_{t}, ΔW_{t}, and W_{t}. During the releasing season, ΔW is calculated as:

$$\Delta W_i = \begin{cases} -W_i \dfrac{(-\Delta W_{\mathrm{t},i})}{W_{\mathrm{t},i}} & \text{if } W_i \le W_{\mathrm{t},i}; \quad\quad (5\mathrm{a}) \\[2ex] \Delta \tilde{W}_i - \left[\left(W_i + \Delta \tilde{W}_i\right) - \left(W_{\mathrm{t},i} + \Delta W_{\mathrm{t},i}\right)\right] & \text{if } W_i > W_{\mathrm{t},i} \text{ and } \Delta \tilde{W}_i > \Delta W_{\mathrm{t},i}; \quad\quad (5\mathrm{b}) \\[2ex] \Delta W_{\mathrm{t},i} - (W_i - W_{\mathrm{t},i}) & \text{if } W_i > W_{\mathrm{t},i} \text{ and } \Delta \tilde{W}_i \le \Delta W_{\mathrm{t},i}. \quad\quad (5\mathrm{c}) \end{cases}$$

Here $\Delta \tilde{W}_i = \alpha Q_i - (\alpha Q_{\mathrm{t},i} - \Delta W_{\mathrm{t},i})$. It is the expected release amount to make river discharge equal to the targeted discharge after reservoir regulation. If current water storage is less than the targeted value (the case of Eq. 5a), the ΔW_i is calculated by the W_i with a proportion of $\Delta W_{\mathrm{t},i}$ over $W_{\mathrm{t},i}$. If the current storage is more than the targeted value (the cases of Eq. 5b and

5c), the reservoir can release more water based on a balance between the targeted water storage change $\Delta W_{t,i}$ and the targeted water storage at the next time step $W_{t,i}$ (represented by $\Delta \tilde{W}_i$). Note that all water storage change variables are negative during the releasing season.

During the recharging season, we can calculate the ΔW_i as:

$$\Delta W_i = \begin{cases} \max\left(W_{t,i} + \Delta W_{t,i} - W_i, 0\right) & \text{if } W_i > W_{t,i}; & \text{(6a)} \\ \Delta W_{t,i} + \left(W_{t,i} - W_i\right) & \text{if } W_i \leq W_{t,i}. & \text{(6b)} \end{cases}$$

If current water storage is larger than the targeted value (Eq. 6a), we will try to recharge a volume of water to make $W_{i+1} = W_{t,i+1}$. If current water storage is less than the targeted value (Eq. 6b), we decide to recharge additional water volume besides the $\Delta W_{t,i}$.

ΔW is then applied as a correction of simulated discharges to generate actual monthly streamflows using the following equation:

$$\hat{Q}_{\text{sim},i} = Q_{\text{sim},i} - \Delta W_i / \alpha. \tag{7}$$

Here $\hat{Q}_{\text{sim}}$ [m^3.s^{-1}] is the simulated discharge with reservoir regulation; Q_{sim} [m^3.s^{-1}] is the simulated monthly discharge. Note that this model is a simplified representation of dam management, because it ignores the direct coupling between water demand and irrigation water supply from the cascade of upstream reservoirs. This approach implies that, with a regulated flow, demands will be able to be satisfied and floods to be avoided without being more explicit. A complete coupling of demand, flood, and reservoir management is difficult to implement in the land surface model in absence of data about the purpose and management strategy of each dam, given different possibly conflicting demand of water for industry and drinking versus cropland irrigation.

Before performing the simulation, we estimate the maximum regulation capacity of each study reservoir in each river sections shown in Fig. 1. Table 1 lists collected information of the main reservoirs on the Yellow River. Only large reservoirs like LongYangXia (LYX), LiuJiaXia (LJX), and XiaoLangDi (XLD) are considered in our model because of their huge $C_{\max}$.

2.2 Sub-section diagnosis

Figure 1 shows the YRB and main gauging stations used in this study. To effectively use Q_{obs} for investigating impacts of irrigation and dam regulation on the discharge of different river sections, we divided the YRB into five sub-sections (R$_i$, $i \in [1,5]$, Fig. 1) with an outlet at each gauging station. Thus we can evaluate the water balance in R$_i$ by:

$$\frac{\Delta \text{TWS}_i}{\Delta t} = P_i - \text{ET}_i + \frac{Q_{\text{in},i} - Q_{\text{out},i}}{A_i}. \tag{8}$$

Where Δt is time interval; ΔTWS_i [mm] is change of total water storage in specific R$_i$; P_i [mm.Δt^{-1}] is precipitation in R$_i$; ET_i [mm.Δt^{-1}] is evapotranspiration in R$_i$; A_i [m^2] is area of R$_i$. $Q_{\text{in},i}$ and $Q_{\text{out},i}$ [m^3.Δt^{-1}] are inflow and outflow respectively. In addition, $q_i = Q_{\text{out},i} - Q_{\text{in},i}$ indicates the contribution of R$_i$ to the river discharge, that is the sub-section discharge. This term can be negative if local water supply (e.g., precipitation and groundwater) cannot meet water demand. A conceptual figure of the water balance of a sub-section is shown at the top left of Fig. 1.

2.3 Datasets

Observed monthly discharges (Q_{obs}) from the gauging stations shown in Fig. 1 are used to evaluate the simulations. Several precipitation (P) and evapotranspiration (ET) datasets were selected to evaluate simulated water budgets in each sub-section. The 0.5° 3-hourly precipitation data from GSWP3 (Global Soil Wetness Project Phase 3) is based on GPCC v6 (Global

5   Precipitation Climatology Centre (Becker et al., 2013)) after bias correction with observations. The MSWEP (Multi-Source Weighted-Ensemble Precipitation) is a 0.25° 3-hourly P product integrating numerous in-situ measurements, satellite observations, and meteorological reanalysis (Beck et al., 2017). Three ET datasets are chosen for their potential ability to capture the effect of irrigation disturbance on ET (Yin et al., 2020) (noted as ET$_{\text{obs}}$). GLEAM v3.2a (Global Land Evaporation Amsterdam Model, (Martens et al., 2017)) provides 0.25° daily ET estimations based on a two-soil layer model in which the top

10   soil moisture is constrained by the ESA CCI (European Space Agency Climate Change Initiative) Soil Moisture observations. The FLUXCOM model (Jung et al., 2009) upscales ET data from a global network of eddy covariance towers measurements into a global 0.5° monthly ET product. Since these towers do not cover irrigated systems, ET from irrigation simulated by the LPJml (Lund-Postam-Jena managed Land) is added to ET from non-irrigated systems. The PKU ET product estimates 0.5° monthly ET by water balances at basin scale integrating FLUXNET observations to diagnose sub-basin patterns by a Multiple

15   Tree Ensemble approach (Zeng et al., 2014).

2.4 Simulation protocol

The 0.5° half-hourly GSWP3 atmospheric forcing (Kim, 2017) was used to drive ORCHIDEE simulations (Yin et al., 2018). A 0.5° map with 15 different Plant Functional Types (PFTs) containing crop sowing area information for the three PFT corresponding to the modeled crop (wheat, maize, and rice) is used, based on China's census data. Crop planting dates for wheat,

20   maize, and rice are derived from spatial interpolation of phenological observations from Chinese Meteorological Administration (Wang et al., 2017). Soil texture map is from Zobler (1986). Two simulation experiments were performed to assess the impacts of irrigation on river discharge: 1) NI: no irrigation; 2) IR: irrigated by available stream water resources. Simulations start from a 20-year spin-up in 1982 to initialize the thermal and hydrological variables. Then simulations were performed from 1982 to 2014 over the YRB.

25   The dam operation simulation starts from 1982 with simulated Q from the IR simulation (Q_{IR}) as input. The initial values of W were set to half of the corresponding C_{max}. Considering potential joint regulation of reservoirs, we firstly estimate the total ΔW of all considered reservoirs by using Q_{IR} at HuaYuanKou (outlet of R$_4$, Fig. 1). Then we estimate the ΔW of LYX and LJX reservoir by using Q_{IR} at LanZhou. The difference between these two ΔW is assumed as the ΔW of XLD reservoir. Simulated ΔW is used to estimate actual monthly discharge ($\hat{Q}_{\text{IR}}$) as Eq. 7 without time lag (Fig. S2). Note that negative $\hat{Q}_{\text{IR}}$

30   may occur at TouDaoGuai and LiJin, because huge water withdrawal in R$_3$ and R$_5$ may result in Q_{IR} less than the $\Delta W/\alpha$ upstream.

Hydrology and
Earth System
Sciences
Discussions

Open Access

EGU

2.5 Evaluation metrics

Four metrics are used to evaluate the performances of simulated monthly Q. The mean-square error (MSE) evaluates the magnitude of errors between simulation and observations. It can be decomposed into three components (Kobayashi and Salam, 2000):

$$\text{MSE} = \frac{1}{n}\sum_{i=1}^{n}(S_i - O_i)^2 = \text{SB} + \text{SDSD} + \text{LCS}. \tag{9}$$

Where S_i and O_i are simulated and observed values, respectively; n is the number of samples. SB (squared bias) is the bias between simulated and observed values. In this study, SB represents the difference between simulated and observed multi-year mean annual Q. SDSD (the squared difference between standard deviation) relates to the mismatch of variation amplitudes between simulated and measured values. It can reflect whether our simulation can capture the seasonality of Q_{obs}. LCS (the lack of correlation weighted by the standard deviation) indicates the mismatch of fluctuation patterns between simulated and observed values, which is equivalent to inter-annual variation of Q in this study. The formulas of these three components and detailed explanation can be found in Kobayashi and Salam (2000).

The second evaluation metric is the Nash-Sutcliffe efficiency (NSE) widely used for hydrological model assessments (Krause et al., 2005). However, NSE is not sensitive to the differences of means and variations between simulated and observed values. Therefore, another metric $d \in [0,1]$, defined as the ratio of MSE and potential error, is used to avoid this limitation. It is calculated as:

$$d = 1 - \frac{\sum_{i=1}^{n}(O_i - S_i)^2}{\sum_{i=1}^{n}\left(|S_i - \bar{O}| + |O_i - \bar{O}|\right)^2}. \tag{10}$$

$d = 1$ indicates perfect fit, while $d = 0$ denotes poor agreement. The NSE combines three independent criteria: correlation coefficient r, bias ratio β, and variability ratio γ (Gupta et al., 2009; Kling et al., 2012). The Euclidean distance of them is proposed as an indicator, called modified Kling-Gupta Efficiency (mKGE $\in (-\infty, 1]$; Gupta et al. (2009); Kling et al. (2012)), which avoids heterogeneous sensitivities of NSE to peak and low flows (Krause et al., 2005; Gupta et al., 2009). mKGE is calculated as,

$$\text{mKGE} = 1 - \sqrt{(1-r)^2 + (1-\beta)^2 + (1-\gamma)^2}, \tag{11}$$

$$\beta = \frac{\mu_S}{\mu_O}; \gamma = \frac{\text{CV}_S}{\text{CV}_O}, \tag{12}$$

where μ [m^3.s^{-1}] and CV [-] are the mean and the coefficient of variation of Q, respectively. These indicators are used for three comparisons: 1) Q_{NI} and Q_{obs}; 2) Q_{IR} and Q_{obs}; 3) $\hat{Q}_{\text{IR}}$ and Q_{obs}.

3 Results

3.1 Hydrological cycles at sub-sectional scale

Figure 2 displays water balances and trends in R_i based on simulated results and observations. P_{GSWP3}, which is consistent with P_{MSWEP}, decreases from $543.6\,\mathrm{mm.yr}^{-1}$ (R_1) to $254.2\,\mathrm{mm.yr}^{-1}$ (R_3), and then rises until $652.1\,\mathrm{mm.yr}^{-1}$ (R_5). The magnitudes

5 of simulated ET (both $\mathrm{ET_{NI}}$ and $\mathrm{ET_{IR}}$) have no significant differences with $\mathrm{ET_{obs}}$ aggregated over sub-sections R_1 to R_5. Except for R_1 where cropland is rare, $\mathrm{ET_{IR}}$ accounts for more than 80% of P_{GSWP3} in the YRB with a maximum value of 96.5% in R_3. The difference between $\mathrm{ET_{IR}}$ and $\mathrm{ET_{NI}}$ is due to the account of irrigation, which accounts for 9.1% and 8.2% of $\mathrm{ET_{NI}}$ in R_3 and R_5 respectively as caused by the large irrigation demand. The impact of irrigation can be detected from sub-sectional discharge ($q_i = (Q_{\mathrm{out},i} - Q_{\mathrm{in},i})/A_i$) as well. For instance, both q_{obs} and q_{IR} are negative in R_3 and R_5, suggesting that local

10 surface water resources cannot meet water usage and upstream discharge is used for irrigation. As irrigation water transfers between grid cells are not represented in our simulations, the non-availability of water locally results in an underestimation of the irrigation amounts explaining why $q_{\mathrm{IR}} > q_{\mathrm{obs}}$ in R_3 to R_5.

The trends of P and ET are positive but not significant in most R_i during the period 1982–2014 (bottom panel of Fig. 2). However, significant trends can be found in both simulated and observed q in some R_i. The decrease of q_{obs} in R_1 is not captured

15 by the model, neither in q_{NI} nor q_{IR}. This underestimated decrease of river discharge might be linked to decreased glacier melt or increased non-irrigation human water withdrawals, which are ignored in our simulations. In R_2 and R_3, the q_{obs} trends are determined by the joint effects of climate change (e.g., P increase) and human water withdrawals. The trends of q_{IR} show the same direction as that of q_{obs}. In R_5 however q_{obs} increased by $1.67\,\mathrm{mm.yr}^{-1}$, which was not captured by the simulation for q_{IR}. Besides P increase shown here, another possible driver of increasing q_{obs} in R_5 is a decrease of water withdrawal due to

20 the improvement of irrigation efficiency (Yin et al., 2020). Moreover, the water use management may play an important role in the observed positive trends of q_{obs} as well, with the aim to increase the streamflow at the downstream of the Yellow River to avoid discharge cutoff ($Q_{\mathrm{obs}} < 1\,\mathrm{m^3.s}^{-1}$) that occurred in 1990's (Wang et al., 2006).

Irrigation not only influences annual discharge in the Yellow River, but also affects its intra-annual variation. In general, the discharge yield, (Y_Q, defined by the sum of surface runoff and drainage) of all grid cells in NI should be higher than that in

25 IR because our irrigation model harvests the stream water reservoirs which is a fraction of drainage and runoff. However, our simulations show that $Y_{Q,\mathrm{NI}}$ can be less than $Y_{Q,\mathrm{IR}}$ (Fig. S3) at the beginning of monsoon season. This is because irrigation keeps soil moisture (SM) higher than SM without irrigation in July in R_4 and R_5 (Fig. S3d and S3e), which in turn promotes Y_Q because the soil water capacity is lower and a larger fraction of P goes to runoff. This mechanism highlighted that irrigation could enhance the heterogeneity of water temporal distribution and may reinforce upcoming floods after a dry season.

30 ### 3.2 Comparison between observed and simulated Q

Figure 3 illustrates time series of annual discharge and of the seasonality of monthly discharge. Our simulations underestimate Q_{obs} at TangNaiHai in R_1 because we miss glacier melt. After LanZhou, the magnitudes of Q_{IR} coincide very well with that of Q_{obs}, indicating that irrigation strongly reduces the annual discharge of Yellow River by as much as 64% until R_5. However,

Hydrology and
Earth System
Sciences
Discussions

Open Access

EGU

the seasonality of monthly Q_{IR} is quite different from that of Q_{obs} (Fig. 3f-3j). Despite a good match between annual Q_{IR} and Q_{obs} our model without dams produces an underestimation of Q in dry season and an overestimation of Q in flood season. Such a mismatch of Q seasonality is likely caused primarily by dam regulation ignored in the model. The locations of several big reservoirs are shown in the bottom panel of Fig. 1 and related information are listed in Table 1. Before the operation of

5   the LongYangXia dam which has a regulation capacity of 193.5×10^8 m^3 (green bar in Fig. 4b), the peaks of monthly Q_{NI} at LanZhou were slightly lower than the peaks of Q_{obs} in R$_2$ (Fig. 4b), as well as the case at TangNaiHai (Fig. 4a), possibly due to lack of glacier melt in the model for this upper sub-section of the YRB in our simulation. But after the construction of the LongYangXia reservoir in 1986, modeled peak Q_{NI} became systematically higher than the peak of Q_{obs} each year, suggesting that the construction of this dam caused the observed peak reduction (Fig. 4b). Moreover, the seasonality of Q_{obs}

10   changed dramatically in period of 1982-2014, but no similar trend was found in monthly P (Fig. S4), suggesting that reservoir regulation is the primary driver of the observed shift in seasonal streamflow variations of the YRB from 1982 to 2014.

    Reservoirs can also affect inter-annual variations of Q as well, although less than the seasonal variation. For instance, TongGuan and XiaoLangDi are two consecutive gauging stations upstream and downstream the reservoir of XiaoLangDi in R$_4$ (Fig. 1). The annual Q_{obs} at the two stations shows different features after the construction of the XiaoLangDi reservoir in

15   1999.

    Figure 5 shows monthly time series of Q_{obs}, Q_{IR}, and $\hat{Q}_{IR}$ (see Sect. 2.1.2) at each gauging station. Discharge fluctuations are successfully improved in $\hat{Q}_{IR}$. Especially the baseflow of $\hat{Q}_{IR}$ coincides well with that of Q_{obs} during winter and spring. The only exception occurs at LiJin, where $\hat{Q}_{IR}$ overestimates the discharge from January to May. In fact, the water release from XLD during this period would be withdrawn for irrigation and industry in R$_5$. However, our offline dam model is not able to

20   simulate the interactions, leading to the overestimation.

    The dam model is successful in flood control as well. At LanZhou, although $\hat{Q}_{IR}$ underestimates the peak flows due to the bias of the simulated mean annual discharge (Fig. 3b), its seasonality is much smoother than that of Q_{IR}. Indeed, such underestimation is also affected by special water management during extreme years. From 2000 to 2002, the YRB experienced severe droughts with 10~15% precipitation less than usual, leading to a decrease of surface water resource as much as 45% (Water

25   Resources Bulletin of China, http://www.mwr.gov.cn/sj/tjgb/szygb/). To guarantee base flow, a set of temporal policies were applied (e.g., reducing water withdrawn, increasing water price, releasing more water from reservoirs, etc). However, those measures are not accounted in the model. Thus higher irrigation demand during drought year promotes the underestimation of the river discharge. From TouDaoGuai to LiJin, the floods from August to October are dramatically reduced by the dam model. Nevertheless, the peaks are still overestimated in $\hat{Q}_{IR}$. It might be due to numerous medium reservoirs ignored by our model

30   (203 medium reservoirs until the end of 2014 (YRCC, 2015)). In our simulation, 326.5×10^8 m^3 regulation capacity is considered, which only accounts for 45% of total storage capacity (720×10^8 m^3 (Ran and Lu, 2012)). Moreover, the five irrigation districts (http://www.yrcc.gov.cn/hhyl/yhgq/, (Tang et al., 2008)), a special irrigation system in the YRB, could contribute to flood reduction. For instance, the Hetao Plateau is the traditional irrigation district. Its hydraulic system can divert river water into its complicated irrigation network ([106.5–109°E]×[40.5–41.5°N] in Fig. 1) by water level difference during the flood

season. This no-dam diversion system at the Hetao Plateau can take $50 \times 10^8 \, \mathrm{m}^3$ from the Yellow River per year, accounting for 14% annual discharge in R_3.

Our simulated ΔW in R_2 is verified by comparing to observations (Jin et al., 2017) (left panel of Fig. 6) suggesting that our simple dam model is able to capture the seasonal variation of ΔW ($r = 0.9$, $p < 0.001$). In the case of XiaoLangDi where the correlation is smaller ($r = 0.34$, $p = 0.28$; right panel of Fig. 6), the mismatch could be explained by sediment regulation procedures, given that this reservoir releases a huge amount of water in June for reservoir cleaning and sediment flushing downstream (Baoligao et al., 2016; Kong et al., 2017; Zhuo et al., 2019), a process not taken into account in our simple dam model. Moreover, because we ignored numerous medium reservoirs, the simulated water recharge during the flood season could be overestimated.

Figure 7 illustrates the model performances with different metrics in different R_i. The results show that MSE increases considerably from R_1 to R_5, implying accumulated impacts of ignored error sources in increasing the error of modeled Q when going downstream in the entire catchment, most likely those error sources are omission errors of anthropogenic factors such as drinking and industrial water removals, but also of natural origin such as the role of riparian wetlands and floodplains (e.g., the Sanshenggong water conservancy hub), and the non-represented small streams in the routing of ORCHIDEE (e.g., the irrigation system at the Hetao Plateau). From the decomposition of MSE, we found that adding irrigation in the model removes most of the bias in the average magnitude Q by reducing the SB error term of MSE. On the other hand, adding the reservoir regulations contribute to improve the phase variations of Q which are dominated by the phase of the seasonal cycle, by reducing the SDSD error term. Nevertheless, the LCS error term indicating the magnitude of the variability, mainly at inter-annual time scales, has no significant improvement with the representation of irrigation and dam regulations. It is because some of reservoirs are able to regulate Q inter-annually (Table 1), which can be observed from Fig. 4c. However, related operation rules are unclear and are not implemented in our dam model. Improvements were found in d as well, which demonstrates that the way human effects on Q of the Yellow River were modeled brings more realistic results, despite ignoring the direct effect of irrigation demand on reservoir release, and ignored industrial and domestic water demands.

The NSEs are improved significantly from R_2 to R_5 by including the effects of irrigation and dams, but the values of this metrics are still negative, reflecting the accumulation of other errors gradually weakening the agreement between $\hat{Q}_{\mathrm{IR}}$ and Q_{obs}. Another important reason of negative NSEs in the $\hat{Q}_{\mathrm{IR}} \sim Q_{\mathrm{obs}}$ comparison is the definition of NSE, which is not tolerant to amplitude of simulated Q exceeding that of observed Q (Fig. 5). As an improved metrics from NSE, the mKGE reveals significant increase after considering dam operations (Fig. 7d). Particularly at LanZhou and HuaYuanKou, the mKGE of $\hat{Q}_{\mathrm{IR}} \sim Q_{\mathrm{obs}}$ increases 0.86 and 1.11 than that of $Q_{\mathrm{IR}} \sim Q_{\mathrm{obs}}$, respectively. Note that the mKGEs of $Q_{\mathrm{IR}} \sim Q_{\mathrm{obs}}$ are smaller than that of $Q_{\mathrm{NI}} \sim Q_{\mathrm{obs}}$ from R_2 to R_4, because irrigation enlarge the intra-annual varaition consequently leading to worse the γ in mKGE (Eq. 11).

4 Discussion

This study validated the performances of the ORCHIDEE land surface model and a simple dam operation model in simulating hydrological processes in the YRB, and quantified the impacts of irrigation and dam operation on the fluctuations of the Yellow River discharge. Simulated hydrological components were compared to observations in different sub-sections with fair agreement (e.g., $4.5 \pm 6.9\%$ for ET). Irrigation mainly affects the magnitude of annual discharges, reducing by about 64% the annual streamflows near the outlet from $2595.6 \, \mathrm{m^3.s^{-1}}$ to $942.1 \, \mathrm{m^3.s^{-1}}$ based on our simulations. As the water of Yellow River is reaching the limit of usage (Feng et al., 2016), we did not find any significant effect of irrigation on streamflow trends. Instead of increasing river water withdrawals, the growing water demand appeared to have been balanced by improving water use efficiency during the study period (Yin et al., 2020; Zhou et al., 2019). Our simulation reveals that the impact of irrigation on streamflow may be positive under special situations, which was also shown in one previous study (Kustu et al., 2011). However, different from the irrigation-ET-precipitation atmospheric feedback mechanisms found by Kustu et al. (2011), we demonstrated that irrigation may significantly increase soil moisture and promote runoff yield during the following wet season. It implies that irrigation in such landscapes may reinforce the magnitude of floods during the rainy season by a higher legacy soil moisture.

Dams strongly regulate the temporal variation of streamflows (Chen et al., 2016; Li et al., 2016; Yaghmaei et al., 2018). By including simple regulation rules depending only on inflows, our dam model explained about 48–77% of the simulation error (MSE in Fig. 7), especially for SDSD which is dominated by seasonal modulation from dams on the river discharge. Moreover, we confirmed that the change of Q_{obs} seasonality during the study period is not due to the climate change (Fig. S4, but is determined by dam operations (Wang et al., 2006).) Different from other dam modules in Global Hydrological Models (GHMs) and Land Surface Models (LSMs) (Biemans et al., 2011; Hanasaki et al., 2006; Wada et al., 2014), our dam model firstly compares the regulation capacity of reservoir with the discharge fluctuations in order to assess the operation targets. This is more realistic because the operation rules do not directly depend on the water demand, but is based on the size of the reservoir. In addition, our dam model does not require any prior knowledge from observations (e.g., observed mean monthly/annual discharge). The advantage of this feature is that we can provide reasonable simulations of dam operations even if biases remain in simulated discharges, which are hardly avoided in models (Hanasaki et al., 2006).

Big dams, like the LongYangXia, LiuJiaXia, and XiaoLangDi, are able to regulate streamflow inter-annually (Wang et al., 2018) in order to smooth the inter-annual distribution of water resources in YRB (Piao et al., 2010; Wang et al., 2006; YRCC, 2015). However, corresponding operation rules are unclear and were not implemented explicitly in the simple dam model. The error corresponding to inter-annual variation (LCS in MSE in Fig. 7) was not reduced by including our simulation of dams. In the dam model, some functions of reservoirs, such as providing irrigation supply, industrial and domestic water, electricity generation, and flood control (Basheer and Elagib, 2018) are not explicitly represented. Particularly the XiaoLangDi dam carries a distinctive water-sediment mission, which scours sediments at downstream of the Yellow River by creating artificial floods in June (Kong et al., 2017; Zhuo et al., 2019). These functions are associated with many socioeconomic factors and drivers leading to competing demands for water (e.g., policies, electricity price, water price, land use change, irrigation

techniques, water management techniques, and dams inter-connection), which could be better understood and implemented into integrated hydrological models to project future water resources dynamics for sustainable development.

Our simulations ignored potential impacts of dams and reservoirs on local climate (Degu et al., 2011). The sum of water area of several artificial reservoirs (LongYangXia, LiuJiaXia, BoHaiWan, SanShengGong, and XiaoLangDi) is approximately

5   $1056\,\mathrm{km}^2$, which is larger than the 10th largest natural lake in China (Lake Zhari Namco with $996.9\,\mathrm{km}^2$ surface area). These water bodies can also significant influence local energy budgets. And Related water loss from reservoir evaporation may be considerable especially in arid and semi-arid area (Friedrich et al., 2018; Shiklomanov, 1999), which should be taken into account in future studies. Besides, the five large irrigation districts (http://www.yrcc.gov.cn/hhyl/yhgq/) could dramatically alter the local climate as well. For instance, the Hetao Plateau takes about $50\times10^8\,\mathrm{m}^3$ from the Yellow River every year

10   during the flood season. Its irrigation area is $5740\,\mathrm{km}^2$ with an evapotranspiration rate ranging between $1200{\sim}1600\,\mathrm{mm.yr}^{-1}$. However, as these irrigation districts divert river water without dams or with multiple medium dams, they are not taken into account in most Yellow River studies. Another non-negligible factor in the case of Yellow River is sedimentation, which reduces the regulation capacities of reservoirs and weakens streamflow regulation by human. For instance, the total capacity of QingTongXia declined from 6.06 to $0.4\times10^8\,\mathrm{m}^3$ since 1978 due to sedimentation. Therefore, how land use change and

15   evolution of natural ecosystems affect sediment load and deposition is another key factor to project dams disturbances on streamflow in the YRB.

Simulating anthropogenic disturbances to river discharge is a challenge. In the case of the Yellow River, well calibrated models can provide accurate natural discharge simulations with NSE as high as 0.9 (Yuan et al., 2016). However, when considering the impacts of irrigation and dams, the performances of simulations are much worse. For instance, the simulation considering

20   anthropogenic effects from Hanasaki et al. (2018) had NSE$=0.11$ at HuaYuanKou, which was even worse than the simulation with only natural processes (NSE$=0.14$). Similarly, Wada et al. (2014) showed NSE decrease after considering anthropogenic factors in the YRB, implying the complexity of modelling human activities. In fact, our simulated patterns are very similar with a set of simulations by GHMs (Fig. S2 from Liu et al. (2019)). Dislike some catchment scale studies, which pursue simulated discharge as accurate as possible under well calibration or by using a suite of observed inputs, our primary aim is to implement

25   related interactive mechanisms in a physical-based land surface model in order to extrapolate our experience for long term projection under climate change. For instance, current study found that the global greening may promote spring evapotranspiration, which may increase heatwave frequency and intensity in the following summer (Lian et al., 2020). To demonstrate the potential impacts of this trend on water resources management, a robust model including not only hydrological processes but also surface energy balances, vegetation dynamics, photosynthesis, and crop phenology is required.

30 **5 Conclusions**

The impacts of irrigation and dam regulation on streamflow fluctuation of the Yellow River were qualified and quantified in this study by using a process-based land surface model and a simple dam operation model. Irrigation mainly contributes to the reduction of annual streamflow by as much as 64%. The change of intra-annual variation of streamflows of the Yellow River

appears not to be caused by climate change, at least not by significant changes of precipitation patterns and land use during the study period, but by the construction of dams and their operation. After considering the impacts of dams, we found that dams regulation can explain about 48–77% of the fluctuations of streamflows. The effect of dams may be still underestimated because we only considered simple regulation rules based on inflows, but ignored its interactions with irrigation demand downstream.

5 Moreover, our analysis showed that several reservoirs on the Yellow River are able to influence streamflows inter-annually. However, such effects are not quantified due to lack of knowledge of the regulation rules across our study period.

References

Baoligao, B. Y., Xu, F. R., Chen, X. R., Wang, X. Y., and Chen, W. X.: Acute impacts of reservoir sediment flushing on fishes in the Yellow River, Journal of Hydro-Environment Research, 13, 26–35, https://doi.org/10.1016/j.jher.2015.11.003, https://linkinghub.elsevier.com/retrieve/pii/S1570644316000022, 2016.

5 Basheer, M. and Elagib, N. A.: Sensitivity of Water-Energy Nexus to dam operation: A Water-Energy Productivity concept, Science of the Total Environment, 616-617, 918–926, https://doi.org/10.1016/j.scitotenv.2017.10.228, http://linkinghub.elsevier.com/retrieve/pii/S0048969717329467, 2018.

Beck, H. E., van Dijk, A. I. J. M., Levizzani, V., Schellekens, J., Miralles, D. G., Martens, B., and de Roo, A.: MSWEP: 3-hourly 0.25° global gridded precipitation (1979–2015) by merging gauge, satellite, and reanalysis data, Hydrology and Earth System Sciences, 21, 589–615,

10 https://doi.org/10.5194/hess-21-589-2017, https://www.hydrol-earth-syst-sci.net/21/589/2017/, 2017.

Becker, A., Finger, P., Meyer-Christoffer, A., Rudolf, B., Schamm, K., Schneider, U., and Ziese, M.: A description of the global land-surface precipitation data products of the Global Precipitation Climatology Centre with sample applications including centennial (trend) analysis from 1901–present, Earth System Science Data, 5, 71–99, https://doi.org/10.5194/essd-5-71-2013, http://www.earth-syst-sci-data.net/5/71/2013/, 2013.

15 Biemans, H., Haddeland, I., Kabat, P., Ludwig, F., Hutjes, R. W. A., Heinke, J., Von Bloh, W., and Gerten, D.: Impact of reservoirs on river discharge and irrigation water supply during the 20th century, Water Resources Research, 47, https://doi.org/10.1029/2009WR008929, http://doi.wiley.com/10.1029/2009WR008929, 2011.

Chen, J., Finlayson, B. L., Wei, T. Y., Sun, Q. L., Webber, M., Li, M. T., and Chen, Z. Y.: Changes in monthly flows in the Yangtze River, China – With special reference to the Three Gorges Dam, Journal of Hydrology, 536, 293–301, https://doi.org/10.1016/j.jhydrol.2016.03.008,

20 http://dx.doi.org/10.1016/j.jhydrol.2016.03.008https://linkinghub.elsevier.com/retrieve/pii/S0022169416301135, 2016.

de Boer, H. J., Eppinga, M. B., Wassen, M. J., and Dekker, S. C.: A critical transition in leaf evolution facilitated the Cretaceous angiosperm revolution, Nature Communications, 3, 1221, https://doi.org/10.1038/ncomms2217, http://www.pubmedcentral.nih.gov/articlerender.fcgi?artid=3514505{&}tool=pmcentrez{&}rendertype=abstracthttp://www.nature.com/doifinder/10.1038/ncomms2217, 2012.

Degu, A. M., Hossain, F., Niyogi, D., Pielke, R., Shepherd, J. M., Voisin, N., and Chronis, T.: The influence of large dams on surrounding

25 climate and precipitation patterns, Geophysical Research Letters, 38, n/a–n/a, https://doi.org/10.1029/2010GL046482, http://doi.wiley.com/10.1029/2010GL046482, 2011.

Feng, X. M., Fu, B. J., Piao, S. L., Wang, S., Ciais, P., Zeng, Z. Z., Lü, Y. H., Zeng, Y., Li, Y., Jiang, X. H., and Wu, B. F.: Revegetation in China's Loess Plateau is approaching sustainable water resource limits, Nature Climate Change, 6, 1019–1022, https://doi.org/10.1038/nclimate3092, http://www.nature.com/doifinder/10.1038/nclimate3092, 2016.

30 Friedrich, K., Grossman, R. L., Huntington, J., Blanken, P. D., Lenters, J., Holman, K. D., Gochis, D., Livneh, B., Prairie, J., Skeie, E., Healey, N. C., Dahm, K., Pearson, C., Finnessey, T., Hook, S. J., and Kowalski, T.: Reservoir Evaporation in the Western United States: Current Science, Challenges, and Future Needs, Bulletin of the American Meteorological Society, 99, 167–187, https://doi.org/10.1175/BAMS-D-15-00224.1, http://journals.ametsoc.org/doi/10.1175/BAMS-D-15-00224.1, 2018.

Grill, G., Lehner, B., Thieme, M., Geenen, B., Tickner, D., Antonelli, F., Babu, S., Borrelli, P., Cheng, L., Crochetiere, H., Ehalt Macedo, H.,

35 Filgueiras, R., Goichot, M., Higgins, J., Hogan, Z., Lip, B., McClain, M. E., Meng, J., Mulligan, M., Nilsson, C., Olden, J. D., Opperman, J. J., Petry, P., Reidy Liermann, C., Sáenz, L., Salinas-Rodríguez, S., Schelle, P., Schmitt, R. J. P., Snider, J., Tan, F., Tockner, K., Valdujo,

P. H., van Soesbergen, A., and Zarfl, C.: Mapping the world's free-flowing rivers, Nature, 569, 215–221, https://doi.org/10.1038/s41586-019-1111-9, http://www.nature.com/articles/s41586-019-1111-9, 2019.

Gupta, H. V., Kling, H., Yilmaz, K. K., and Martinez, G. F.: Decomposition of the mean squared error and NSE performance criteria: Implications for improving hydrological modelling, Journal of Hydrology, 377, 80–91, https://doi.org/10.1016/j.jhydrol.2009.08.003, http://dx.doi.org/10.1016/j.jhydrol.2009.08.003https://linkinghub.elsevier.com/retrieve/pii/S0022169409004843, 2009.

Haddeland, I., Heinke, J., Biemans, H., Eisner, S., Flörke, M., Hanasaki, N., Konzmann, M., Ludwig, F., Masaki, Y., Schewe, J., Stacke, T., Tessler, Z. D., Wada, Y., and Wisser, D.: Global water resources affected by human interventions and climate change, Proceedings of the National Academy of Sciences, 111, 3251–3256, https://doi.org/10.1073/pnas.1222475110, http://www.pnas.org/lookup/doi/10.1073/pnas.1222475110, 2014.

Hanasaki, N., Kanae, S., and Oki, T.: A reservoir operation scheme for global river routing models, Journal of Hydrology, 327, 22–41, https://doi.org/10.1016/j.jhydrol.2005.11.011, https://linkinghub.elsevier.com/retrieve/pii/S0022169405005962, 2006.

Hanasaki, N., Fujimori, S., Yamamoto, T., Yoshikawa, S., Masaki, Y., Hijioka, Y., Kainuma, M., Kanamori, Y., Masui, T., Takahashi, K., and Kanae, S.: A global water scarcity assessment under Shared Socio-economic Pathways - Part 2: Water availability and scarcity, Hydrology and Earth System Sciences, 17, 2393–2413, https://doi.org/10.5194/hess-17-2393-2013, https://www.hydrol-earth-syst-sci.net/17/2393/2013/, 2013.

Hanasaki, N., Yoshikawa, S., Pokhrel, Y., and Kanae, S.: A global hydrological simulation to specify the sources of water used by humans, Hydrology and Earth System Sciences, 22, 789–817, https://doi.org/10.5194/hess-22-789-2018, https://www.hydrol-earth-syst-sci.net/22/789/2018/, 2018.

Intergovernmental Panel on Climate Change: Fifth Assessment Report of the Intergovernmental Panel on Climate Change, Tech. rep., World Meteorological Organization, 2014.

Jin, S. Y., Zhang, P., and Zhao, W. R.: Analysis of flow process variation degree and influencing factors in inner Mongolia reach of the Yellow River, IOP Conference Series: Earth and Environmental Science, 69, 012 015, https://doi.org/10.1088/1755-1315/69/1/012015, http://stacks.iop.org/1755-1315/69/i=1/a=012015?key=crossref.77e9b258768dfe7eb97dc4049c4fa6f0, 2017.

Jung, M., Reichstein, M., and Bondeau, A.: Towards global empirical upscaling of FLUXNET eddy covariance observations: Validation of a model tree ensemble approach using a biosphere model, Biogeosciences, 6, 2001–2013, https://doi.org/10.5194/bg-6-2001-2009, http://www.biogeosciences.net/6/2001/2009/, 2009.

Kim, H.: Global Soil Wetness Project Phase 3 Atmospheric Boundary Conditions (Experiment 1) [Data set], https://doi.org/10.20783/DIAS.501, 2017.

Kling, H., Fuchs, M., and Paulin, M.: Runoff conditions in the upper Danube basin under an ensemble of climate change scenarios, Journal of Hydrology, 424-425, 264–277, https://doi.org/10.1016/j.jhydrol.2012.01.011, https://linkinghub.elsevier.com/retrieve/pii/S0022169412000431, 2012.

Kobayashi, K. and Salam, M. U.: Comparing Simulated and Measured Values Using Mean Squared Deviation and its Components, Agronomy Journal, 92, 345, https://doi.org/10.1007/s100870050043, http://link.springer.de/link/service/journals/10087/bibs/0092002/00920345.htm, 2000.

Kong, D. X., Miao, C. Y., Wu, J. W., Borthwick, A. G. L., Duan, Q. Y., and Zhang, X. M.: Environmental impact assessments of the Xiaolangdi Reservoir on the most hyperconcentrated laden river, Yellow River, China, Environmental Science and Pollution Research, 24, 4337–4351, https://doi.org/10.1007/s11356-016-7975-4, http://dx.doi.org/10.1007/s11356-016-7975-4http://link.springer.com/10.1007/s11356-016-7975-4, 2017.

Krause, P., Boyle, D. P., and Bäse, F.: Comparison of different efficiency criteria for hydrological model assessment, Advances in Geosciences, 5, 89–97, https://doi.org/10.5194/adgeo-5-89-2005, http://www.adv-geosci.net/5/89/2005/, 2005.

Kustu, M. D., Fan, Y., and Rodell, M.: Possible link between irrigation in the U.S. High Plains and increased summer streamflow in the Midwest, Water Resources Research, 47, https://doi.org/10.1029/2010WR010046, http://doi.wiley.com/10.1029/2010WR010046, 2011.

5 Li, C., Yang, S. Y., Lian, E. G., Yang, C. F., Deng, K., and Liu, Z. F.: Damming effect on the Changjiang (Yangtze River) river water cycle based on stable hydrogen and oxygen isotopic records, Journal of Geochemical Exploration, 165, 125–133, https://doi.org/10.1016/j.gexplo.2016.03.006, http://dx.doi.org/10.1016/j.gexplo.2016.03.006https://linkinghub.elsevier.com/retrieve/pii/S0375674216300656, 2016.

Lian, X., Piao, S. L., Li, L. Z. X., Li, Y., Huntingford, C., Ciais, P., Cescatti, A., Janssens, I. A., Peñuelas, J., Buermann, W., Chen, A. P.,
10 Li, X. Y., Myneni, R. B., Wang, X. H., Wang, Y. L., Yang, Y. T., Zeng, Z. Z., Zhang, Y. Q., and McVicar, T. R.: Summer soil drying exacerbated by earlier spring greening of northern vegetation, Science Advances, 6, https://doi.org/10.1126/sciadv.aax0255, 2020.

Liu, J. G., Zhao, D. D., Gerbens-Leenes, P. W., and Guan, D. B.: China's rising hydropower demand challenges water sector, Scientific Reports, 5, 11 446, https://doi.org/10.1038/srep11446, http://dx.doi.org/10.1038/srep11446http://www.nature.com/articles/srep11446, 2015.

Liu, J. G., Yang, H., Gosling, S. N., Kummu, M., Flörke, M., Pfister, S., Hanasaki, N., Wada, Y., Zhang, X. X., Zheng, C. M., Alcamo, J., and
15 Oki, T.: Water scarcity assessments in the past, present, and future, Earth's Future, 5, 545–559, https://doi.org/10.1002/2016EF000518, http://doi.wiley.com/10.1002/2016EF000518, 2017.

Liu, L. L. and Du, J. J.: Documented changes in annual runoff and attribution since the 1950s within selected rivers in China, Advances in Climate Change Research, 8, 37–47, https://doi.org/10.1016/j.accre.2017.03.005, https://linkinghub.elsevier.com/retrieve/pii/S167492781630065X, 2017.

20 Liu, X. C., Liu, W. F., Yang, H., Tang, Q. H., Flörke, M., Masaki, Y., Müller Schmied, H., Ostberg, S., Pokhrel, Y., Satoh, Y., and Wada, Y.: Multimodel assessments of human and climate impacts on mean annual streamflow in China, Hydrology and Earth System Sciences, 23, 1245–1261, https://doi.org/10.5194/hess-23-1245-2019, https://www.hydrol-earth-syst-sci.net/23/1245/2019/, 2019.

Martens, B., Miralles, D. G., Lievens, H., van der Schalie, R., de Jeu, R. A. M., Fernández-Prieto, D., Beck, H. E., Dorigo, W. A., and Verhoest, N. E. C.: GLEAM v3: satellite-based land evaporation and root-zone soil moisture, Geoscientific Model Devel-
25 opment, 10, 1903–1925, https://doi.org/10.5194/gmd-10-1903-2017, http://www.geosci-model-dev-discuss.net/gmd-2016-162/https://www.geosci-model-dev.net/10/1903/2017/, 2017.

Ngo-Duc, T., Laval, K., Ramillien, G., Polcher, J., and Cazenave, A.: Validation of the land water storage simulated by Organising Carbon and Hydrology in Dynamic Ecosystems (ORCHIDEE) with Gravity Recovery and Climate Experiment (GRACE) data, Water Resources Research, 43, 1–8, https://doi.org/10.1029/2006WR004941, 2007.

30 Piao, S., Friedlingstein, P., Ciais, P., de Noblet-Ducoudre, N., Labat, D., and Zaehle, S.: Changes in climate and land use have a larger direct impact than rising CO2 on global river runoff trends, Proceedings of the National Academy of Sciences, 104, 15 242–15 247, https://doi.org/10.1073/pnas.0707213104, http://www.pnas.org/cgi/doi/10.1073/pnas.0707213104, 2007.

Piao, S. L., Ciais, P., Huang, Y., Shen, Z. H., Peng, S. S., Li, J. S., Zhou, L. P., Liu, H. Y., Ma, Y. C., Ding, Y. H., Friedlingstein, P., Liu, C. Z., Tan, K., Yu, Y. Q., Zhang, T. Y., and Fang, J. Y.: The impacts of climate change on water resources and agriculture in
35 China, Nature, 467, 43–51, https://doi.org/10.1038/nature09364, http://www.ncbi.nlm.nih.gov/pubmed/20811450http://www.nature.com/doifinder/10.1038/nature09364, 2010.

Ran, L. S. and Lu, X. X.: Delineation of reservoirs using remote sensing and their storage estimate: An example of the Yellow River basin, China, Hydrological Processes, 26, 1215–1229, https://doi.org/10.1002/hyp.8224, http://doi.wiley.com/10.1002/hyp.8224, 2012.

Seneviratne, S. I., Donat, M. G., Mueller, B., and Alexander, L. V.: No pause in the increase of hot temperature extremes, Nature Climate Change, 4, 161–163, https://doi.org/10.1038/nclimate2145, http://dx.doi.org/10.1038/nclimate2145http://www.nature.com/doifinder/10.1038/nclimate2145, 2014.

Sherwood, S. and Fu, Q.: A Drier Future?, Science, 343, 737–739, https://doi.org/10.1126/science.1247620, http://www.sciencemag.org/cgi/doi/10.1126/science.1247620, 2014.

Shiklomanov, I. A.: State Hydrological Institute (SHL. St. Petersburg) and United Nations Educational, Scientific and Cultural Organisation, 1999.

Tang, Q. H., Oki, T., Kanae, S., and Hu, H. P.: Hydrological Cycles Change in the Yellow River Basin during the Last Half of the Twentieth Century, Journal of Climate, 21, 1790–1806, https://doi.org/10.1175/2007JCLI1854.1, http://journals.ametsoc.org/doi/abs/10.1175/2007JCLI1854.1, 2008.

Wada, Y., Wisser, D., and Bierkens, M. F. P.: Global modeling of withdrawal, allocation and consumptive use of surface water and groundwater resources, Earth System Dynamics, 5, 15–40, https://doi.org/10.5194/esd-5-15-2014, http://www.earth-syst-dynam.net/5/15/2014/, 2014.

Wada, Y., de Graaf, I. E. M., and van Beek, L. P. H.: High-resolution modeling of human and climate impacts on global water resources, Journal of Advances in Modeling Earth Systems, 8, 735–763, https://doi.org/10.1002/2015MS000618, http://doi.wiley.com/10.1002/2015MS000618, 2016.

Wang, H. J., Yang, Z. S., Saito, Y., Liu, J. P., and Sun, X. X.: Interannual and seasonal variation of the Huanghe (Yellow River) water discharge over the past 50 years: Connections to impacts from ENSO events and dams, Global and Planetary Change, 50, 212–225, https://doi.org/10.1016/j.gloplacha.2006.01.005, https://linkinghub.elsevier.com/retrieve/pii/S0921818106000178, 2006.

Wang, S. S., Mo, X. G., Liu, S. X., Lin, Z. H., and Hu, S.: Validation and trend analysis of ECV soil moisture data on cropland in North China Plain during 1981–2010, International Journal of Applied Earth Observation and Geoinformation, 48, 110–121, https://doi.org/10.1016/j.jag.2015.10.010, http://www.sciencedirect.com/science/article/pii/S0303243415300441http://linkinghub.elsevier.com/retrieve/pii/S0303243415300441, 2016.

Wang, X. H.: Impacts of environmental change on rice ecosystems in China: development, optimization and application of ORCHIDEE-CROP model, Ph.D. thesis, Peking University, 2016.

Wang, X. H., Ciais, P., Li, L., Ruget, F., Vuichard, N., Viovy, N., Zhou, F., Chang, J. F., Wu, X. C., Zhao, H. F., and Piao, S. L.: Management outweighs climate change on affecting length of rice growing period for early rice and single rice in China during 1991–2012, Agricultural and Forest Meteorology, 233, 1–11, https://doi.org/10.1016/j.agrformet.2016.10.016, http://linkinghub.elsevier.com/retrieve/pii/S0168192316304087, 2017.

Wang, X. J., Engel, B., Yuan, X. M., and Yuan, P. X.: Variation Analysis of Streamflows from 1956 to 2016 Along the Yellow River, China, Water, 10, 1231, https://doi.org/10.3390/w10091231, http://www.mdpi.com/2073-4441/10/9/1231, 2018.

Wu, X. C., Vuichard, N., Ciais, P., Viovy, N., de Noblet-Ducoudré, N., Wang, X. H., Magliulo, V., Wattenbach, M., Vitale, L., Di Tommasi, P., Moors, E. J., Jans, W., Elbers, J., Ceschia, E., Tallec, T., Bernhofer, C., Grünwald, T., Moureaux, C., Manise, T., Ligne, A., Cellier, P., Loubet, B., Larmanou, E., and Ripoche, D.: ORCHIDEE-CROP (v0), a new process-based agro-land surface model: model description and evaluation over Europe, Geoscientific Model Development, 9, 857–873, https://doi.org/10.5194/gmd-9-857-2016, http://www.geosci-model-dev-discuss.net/8/4653/2015/http://www.geosci-model-dev.net/9/857/2016/, 2016.

Xi, Y., Peng, S. S., Ciais, P., Guimberteau, M., Li, Y., Piao, S. L., Wang, X. H., Polcher, J., Yu, J. S., Zhang, X. Z., Zhou, F., Bo, Y., Ottle, C., and Yin, Z.: Contributions of Climate Change, CO_2, Land-Use Change, and Human Activities to Changes in River Flow across

10 Chinese Basins, Journal of Hydrometeorology, 19, 1899–1914, https://doi.org/10.1175/JHM-D-18-0005.1, http://journals.ametsoc.org/doi/10.1175/JHM-D-18-0005.1, 2018.

Yaghmaei, H., Sadeghi, S. H., Moradi, H., and Gholamalifard, M.: Effect of Dam operation on monthly and annual trends of flow discharge in the Qom Rood Watershed, Iran, Journal of Hydrology, 557, 254–264, https://doi.org/10.1016/j.jhydrol.2017.12.039, http://linkinghub.elsevier.com/retrieve/pii/S0022169417308570, 2018.

Yin, Z., Ottlé, C., Ciais, P., Guimberteau, M., Wang, X. H., Zhu, D., Maignan, F., Peng, S. S., Piao, S. L., Polcher, J., Zhou, F., and Kim, H.: Evaluation of ORCHIDEE-MICT-simulated soil moisture over China and impacts of different atmospheric forcing data, Hydrology and Earth System Sciences, 22, 5463–5484, https://doi.org/10.5194/hess-22-5463-2018, https://www.hydrol-earth-syst-sci-discuss.net/hess-2017-699/https://www.hydrol-earth-syst-sci.net/22/5463/2018/, 2018.

Yin, Z., Wang, X. H., Ottlé, C., Zhou, F., Guimberteau, M., Peng, S. S., Piao, S. L., Li, L., Bo, Y., Chen, X. L., Zhou, X. D., Kim, H., and Ciais, P.: Improvement of the irrigation scheme in the ORCHIDEE land surface model and impacts of irrigation on regional water budgets over China, accepted, JAMES, 2020.

YRCC: Yellow River Water Resources Bulletin 2014, Tech. rep., Yellow River Conservancy Commission, Zhengzhou, 2015.

Yuan, X., Ma, F., Wang, L. Y., Zheng, Z. Y., Ma, Z. G., Ye, A. Z., and Peng, S. M.: An experimental seasonal hydrological forecasting system over the Yellow River basin – Part 1: Understanding the role of initial hydrological conditions, Hydrology and Earth System Sciences, 20, 2437–2451, https://doi.org/10.5194/hess-20-2437-2016, 2016.

Yuan, X., Jiao, Y., Yang, D., and Lei, H.: Reconciling the Attribution of Changes in Streamflow Extremes From a Hydroclimate Perspective, Water Resources Research, 54, 3886–3895, https://doi.org/10.1029/2018WR022714, 2018.

Zeng, Z. Z., Wang, T., Zhou, F., Ciais, P., Mao, J. F., Shi, X. Y., and Piao, S. L.: A worldwide analysis of spatiotemporal changes in water balance-based evapotranspiration from 1982 to 2009, Journal of Geophysical Research: Atmospheres, 119, 1186–1202, https://doi.org/10.1002/2013JD020941, http://doi.wiley.com/10.1002/2013JD020941, 2014.

Zhou, F., Bo, Y., Ciais, P., Dumas, P., Tang, Q. H., Wang, X. H., Liu, J. G., Zheng, C. M., Polcher, J., Yin, Z., Guimberteau, M., Peng, S. S., Ottle, C., Zhao, X. N., Zhao, J. S., Tan, Q., Chen, L., Shen, H. Z., Yang, H., Piao, S. L., Wang, H., and Y., W.: Deceleration of China's human water use and its socioeconomic drivers, in revision, PNAS, 2019.

Zhu, Z. C., Piao, S. L., Myneni, R. B., Huang, M. T., Zeng, Z. Z., Canadell, J. G., Ciais, P., Sitch, S., Friedlingstein, P., Arneth, A., Cao, C. X., Cheng, L., Kato, E., Koven, C., Li, Y., Lian, X., Liu, Y. W., Liu, R., Mao, J. F., Pan, Y. Z., Peng, S. S., Peñuelas, J., Poulter, B., Pugh, T. A. M., Stocker, B. D., Viovy, N., Wang, X. H., Wang, Y. P., Xiao, Z. Q., Yang, H., Zaehle, S., and Zeng, N.: Greening of the Earth and its drivers, Nature Climate Change, 6, 791–795, https://doi.org/10.1038/nclimate3004, http://www.nature.com/doifinder/10.1038/nclimate3004, 2016.

Zhuo, L., Hoekstra, A. Y., Wu, P., and Zhao, X. N.: Monthly blue water footprint caps in a river basin to achieve sustainable water consumption: The role of reservoirs, Science of the Total Environment, 650, 891–899, https://doi.org/10.1016/j.scitotenv.2018.09.090, https://doi.org/10.1016/j.scitotenv.2018.09.090, 2019.

Zobler, L.: A world soil file for global climate modeling, Tech. rep., NASA Tech, 1986.

Zscheischler, J., Westra, S., van den Hurk, B. J. J. M., Seneviratne, S. I., Ward, P. J., Pitman, A., AghaKouchak, A., Bresch, D. N., Leonard, M., Wahl, T., and Zhang, X. B.: Future climate risk from compound events, Nature Climate Change, 8, 469–477, https://doi.org/10.1038/s41558-018-0156-3, http://dx.doi.org/10.1038/s41558-018-0156-3http://www.nature.com/articles/s41558-018-0156-3, 2018.

Tables

Table 1. Information of artificial reservoirs on the Yellow River with considerable total capacity.

Name	Total capacity (10^8 m^3)	Regulation capacity (10^8 m^3)	Regulation since	Regulation type
LongYangXia	247	193.53	Oct 1986	Inter-annual
LiJiaXia	16.5	–	Dec 1996	Daily, weekly
GongBoXia	6.2	0.75	Aug 2004	Daily
LiuJiaXia	57	41.5	Oct 1968	Inter-annual
YanGuoXia	2.2	–	Mar 1961	Daily
BaPanXia	0.49	0.09	–	Daily
QingTongXia	6.06–0.4*	–	1968	Daily
XiaoLangDi	126.5	91.5	1999	Inter-annual

* The total capacity shrink is due to sedimentation.

Table 2. Values of C_{dam}, Q_{base}, and Q_{peak} used in the dam regulation simulation.

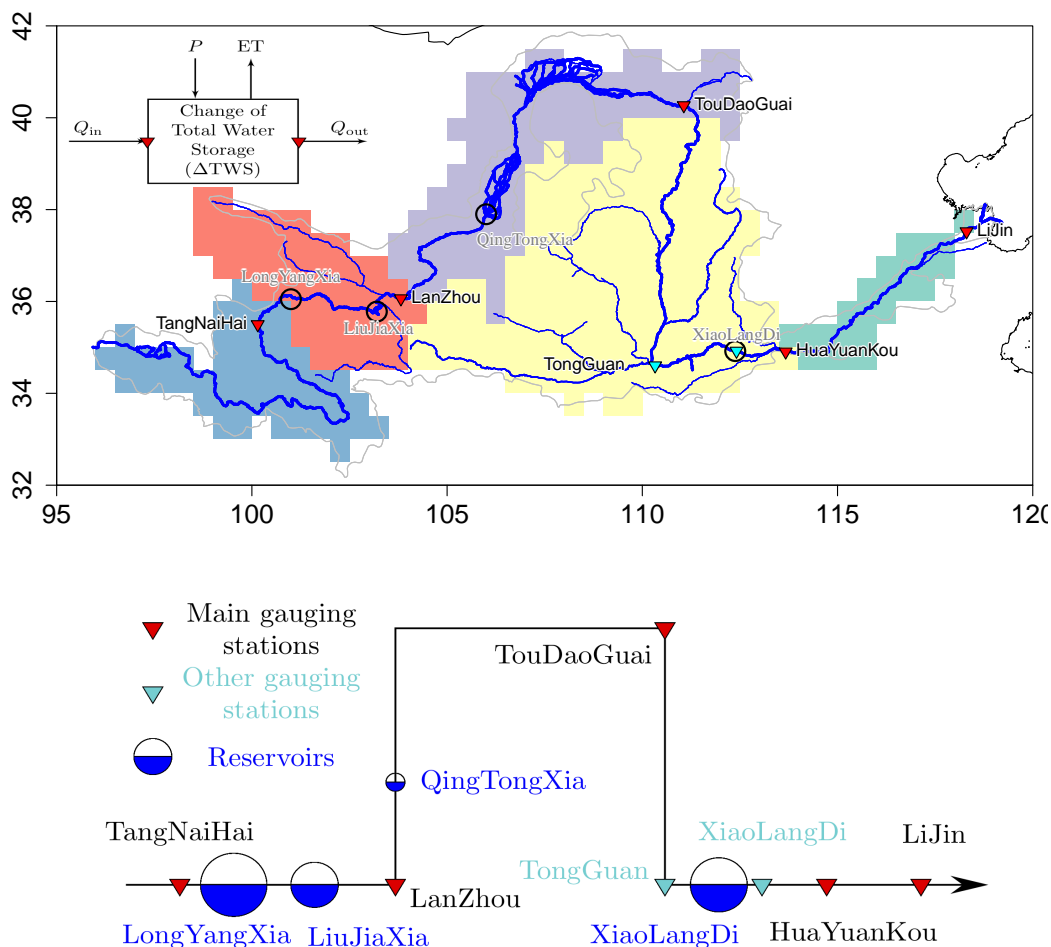| Sub-section	Stations	C_{dam} (10^8 m^3)	Regulation since	Q_{base} (m^3.s^{-1})	Q_{peak} (m^3.s^{-1})
R$_1$	–	–	–	–	–
	TangNaiHai			–	–
R$_2$	TangNaiHai	41.5 before 1987;	1982	–	–
	LanZhou	235 after 1987		423.8	1392.5
R$_3$	LanZhou	–	1982	–	–
	TouDaoGuai			156.5	966.0
R$_4$	TouDaoGuai	91.5	1999	–	–
	HuaYuanKou			295.3	1742.5
R$_5$	HuaYuanKou	–	–	–	–
	LiJin			–	–

Figure 1. Top panel: map of Yellow River Basin. Gray and blue lines indicate the catchment and network of Yellow River based on GIS data, respectively. Dark circles are main artificial reservoirs on the Yellow River. Triangles are gauging stations. Red triangles are main stations used for classifying sub-section and simulation comparison, and teal triangles are stations used to assess the impacts of XiaoLangDi Reservoir on river discharge. Colored patterns are sub-sections between two neighbouring gauging stations based on ORCHIDEE routing map. The water balances of specific sub-section are shown at the top left. Bottom panel: conceptual figure of Yellow River main stream, gauging stations, and artificial reservoirs. The sizes of circles indicate the regulation capacities of these reservoirs (Table 2).

Hydrology and
Earth System
Sciences
Open Access
Discussions
EGU
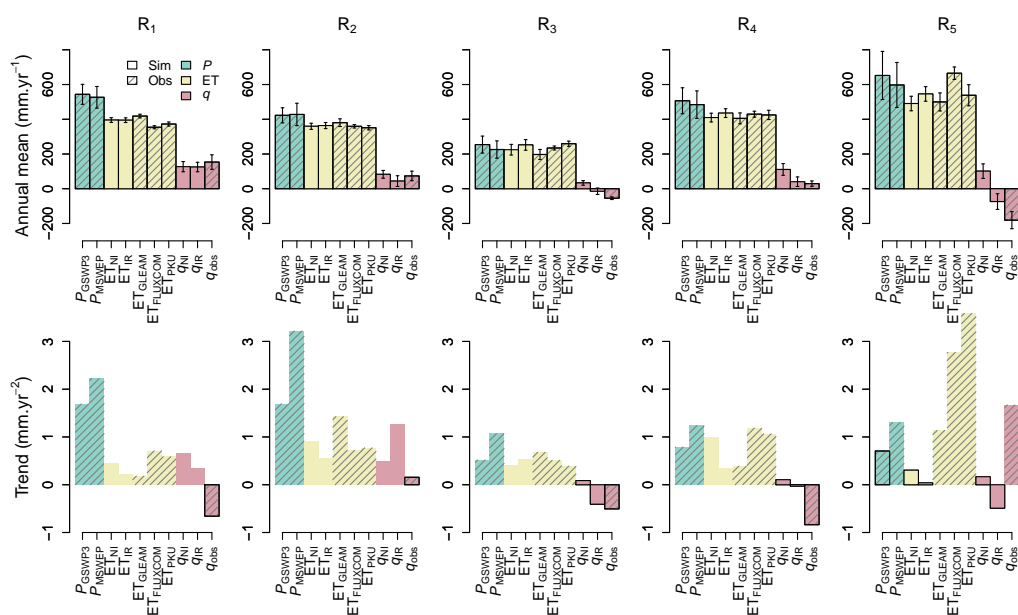
Figure 2. Top panel: Annual mean of hydrological elements in each sub-section of the Yellow River basin from both simulation (plain colors) and observation (hatched colors). Error bars represent for standard deviation. Bottom panel: trends of these elements in each sub-section. Dark borders indicate the trend is statistical significant (p-value < 0.05) according to Mann-Kendall test.
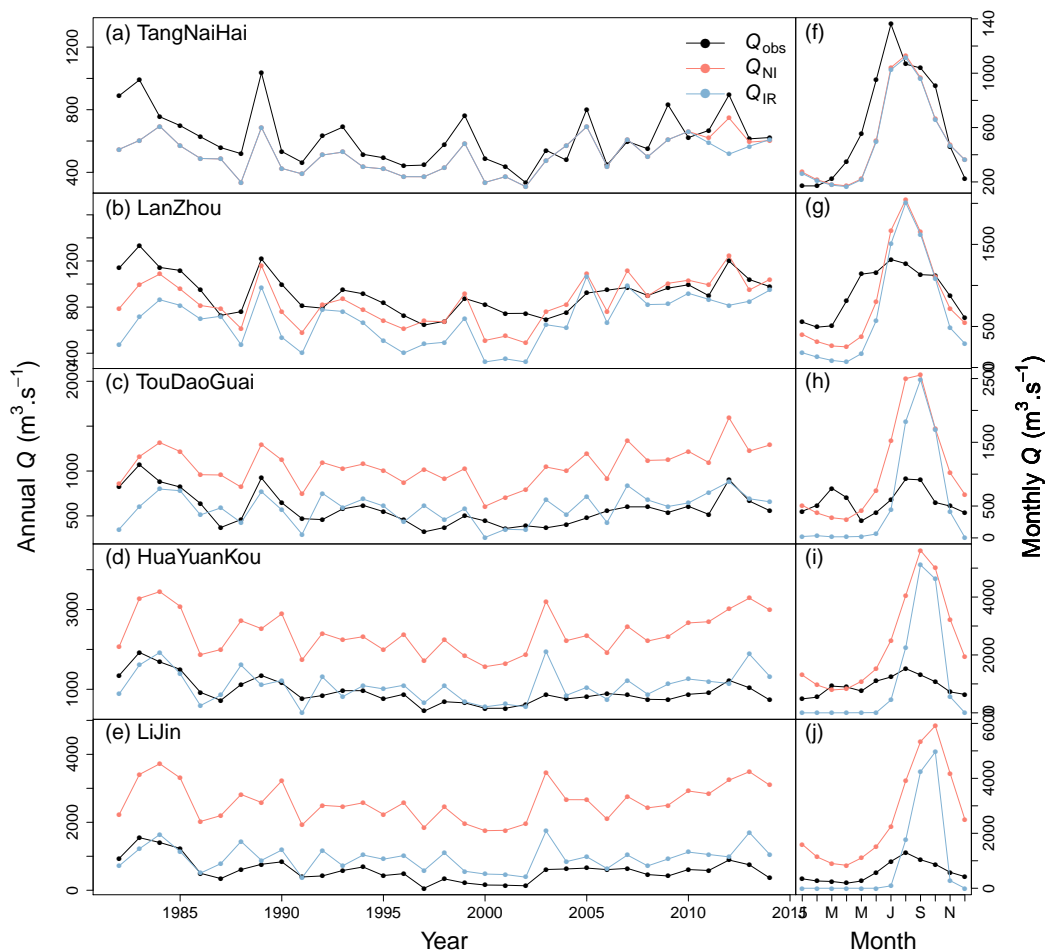
Figure 3. (a)-(e): Time series of annual discharge from observations and simulations at each gauging station. (f)-(j): Seasonality of observed and simulated discharge at each gauging station. Q_{obs} is observed annual mean discharge. Q_{NI} and Q_{IR} are simulated annual mean discharges based on the NI and IR simulations (Sect. 2.4), respectively. These simulations do not account for dams and therefore the seasonality has a higher amplitude than observed in the right hand plots.
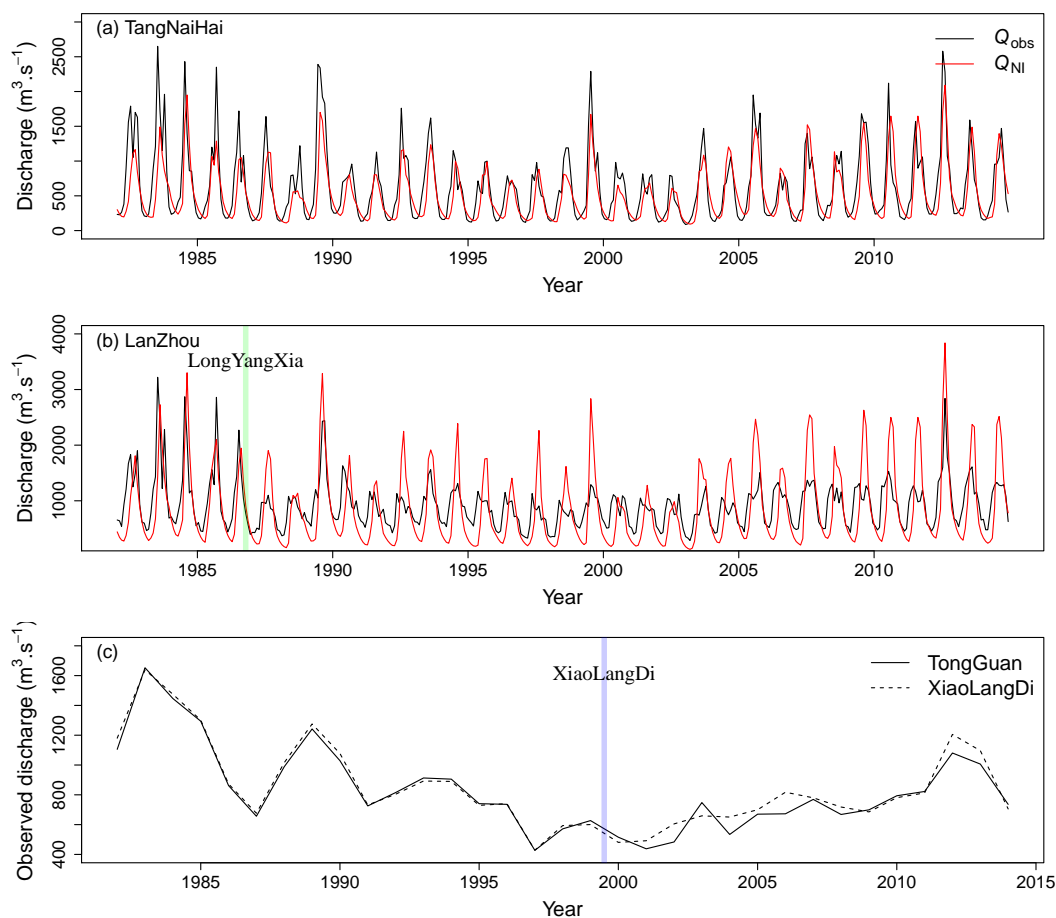
Figure 4. (a)-(b): monthly observed (Q_{obs}) and simulated (Q_{NI}) discharge at TangNaiHai and LanZhou stations. Green bar in (b) indicates the start of the LongYangXia dam regulation. (c): Observed annual discharge at TongGuan and XiaoLangDi gauging stations, which locate at up and down stream of the XiaoLangDi reservoir, respectively (see Fig. 1). Blue bar in (c) indicates the start of the XiaoLangDi dam regulation.
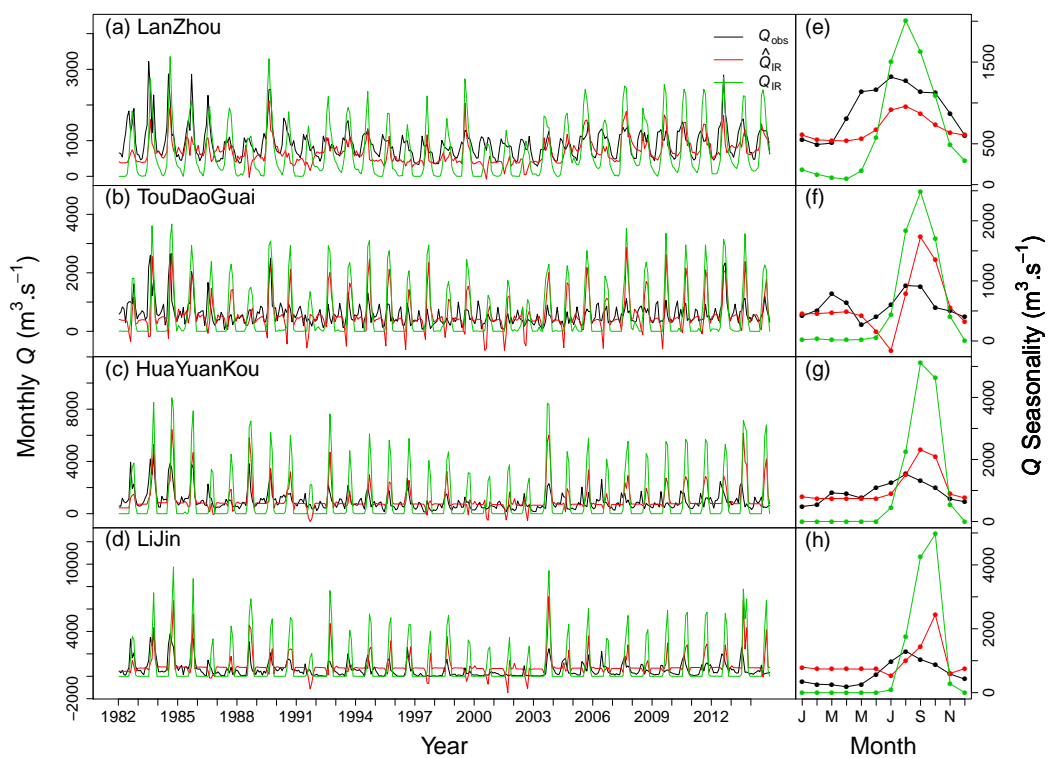
Figure 5. Comparison between observed and simulated actual monthly discharge at gauging stations. Q_{obs} (dark lines) is observed monthly discharge. Q_{IR} (green lines) is simulated monthly discharge from the IR experiment (Sect. 2.4). $\hat{Q}_{IR}$ (red lines) is simulated monthly discharge including impacts of reservoir regulation (Sect. 2.4).
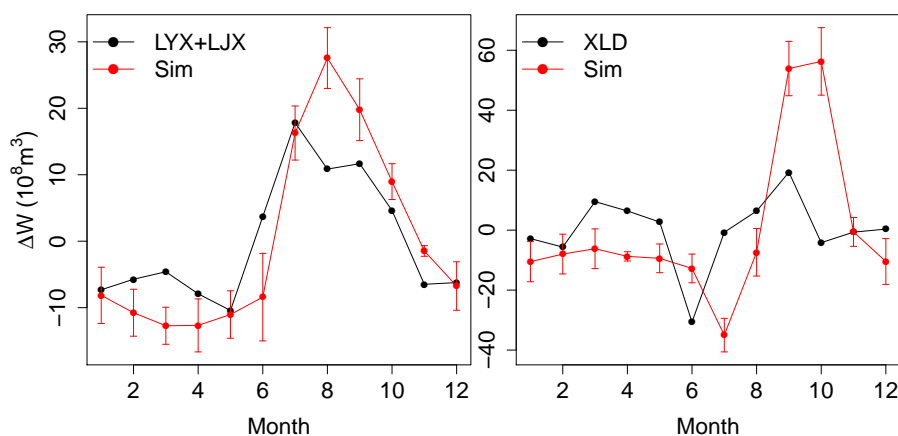
Figure 6. The changes of water storage of dams (ΔW) in R_2 and R_4. The dark line represents the ΔW from literature. The multi-year mean of ΔW of LongYangXi and LiuJiaXia is from Jin et al. (2017). The ΔW of XiaoLangDi is from one year record reported in Kong et al. (2017). Red lines represent corresponding simulated ΔW from our dam regulation model.
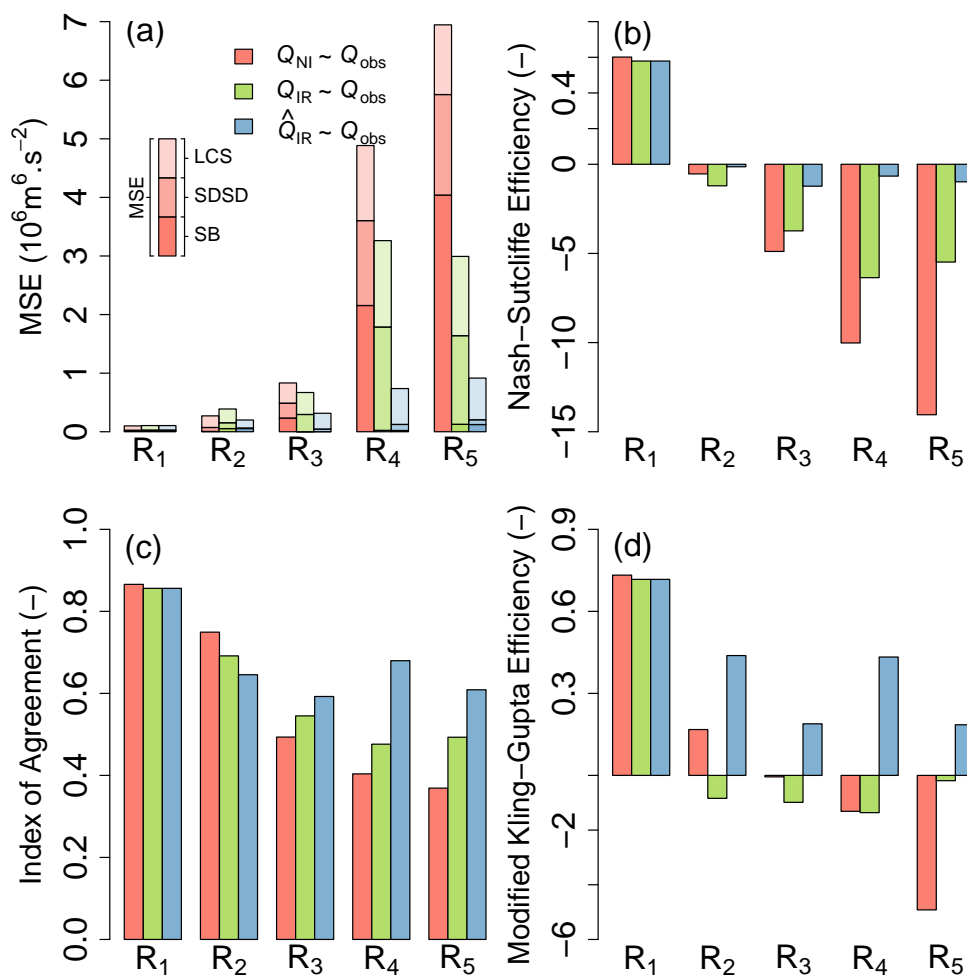
Figure 7. Indicators of Q comparisons in each sub-section of Yellow River Basin. Colors indicate different comparisons. The MSE is decomposed to SB, SDSD, and LCS, which are distinguished by different transparencies.